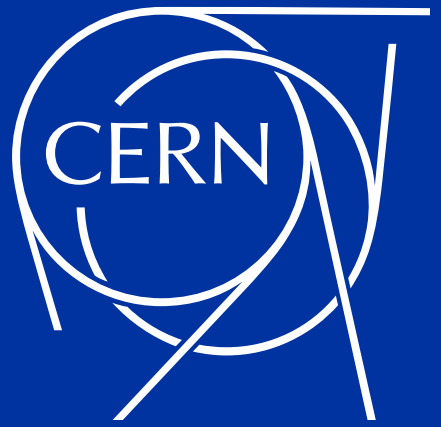

Higgs property measurements (mass, width, CP) with the ATLAS detector

Sébastien Rettie, on behalf of the ATLAS collaboration

12th Edition of the Large Hadron Collider Physics Conference, 4 June 2024

Introduction & motivation

- Rich Higgs boson phenomenology probed by LHC experiments
- Many opportunities to test the validity of Standard Model (SM) predictions and look for new physics
- Achieved observation of main production modes (WH and ZH observed in 2020) and decay modes, and measured several properties e.g. coupling to other particles

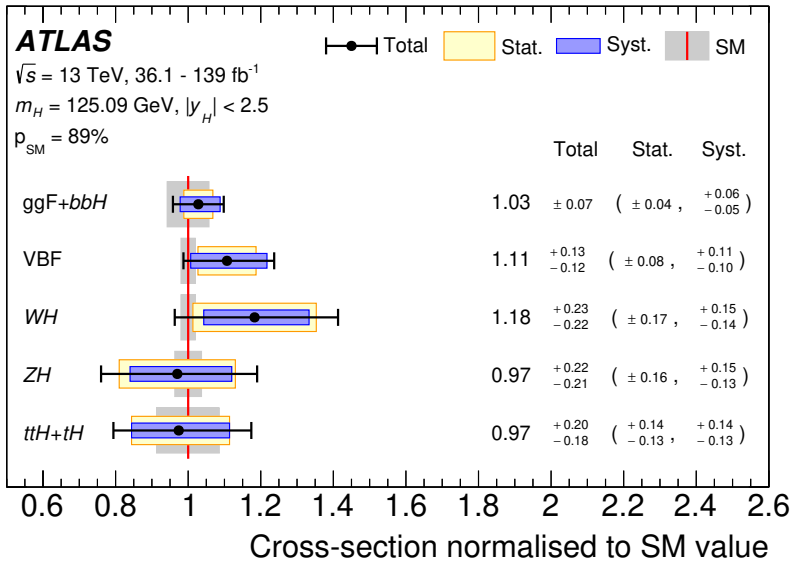

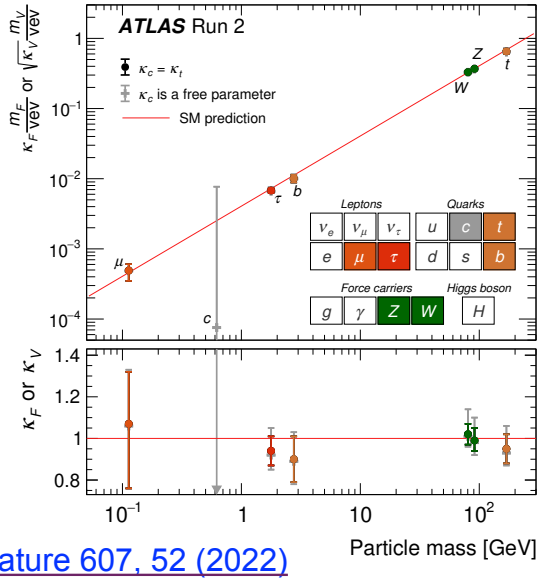

Nature 607, 52 (2022)

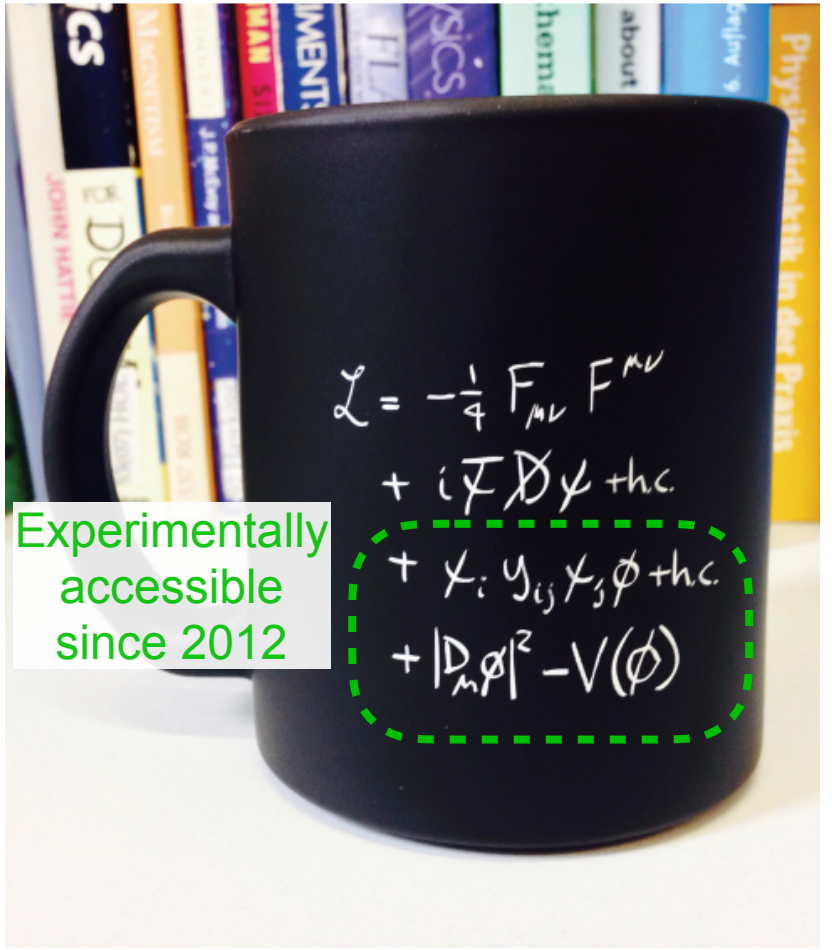

- So far, measurements are consistent with the SM Higgs boson
- Next steps: increase precision, combinations, differential measurements

Overview

- Mass: free parameter that needs to be measured and depends on the Higgs potential parameters
  - PLB 843 (2023) 137880: $H \to ZZ^* \to 4\ell$
  - PLB 847 (2023) 138315: $H \to \gamma\gamma$
  - PRL 131 (2023) 251802: Combination
- Width: predicted SM width is 4.1 MeV and accessible with off-shell production
  - PLB 846 (2023) 138223: $H^* \to ZZ$ off-shell production
- CP: Higgs sector CP violation could help explain observed baryon asymmetry in our Universe
  - JHEP 05 (2024) 105: $H \to ZZ^* \to 4\ell$

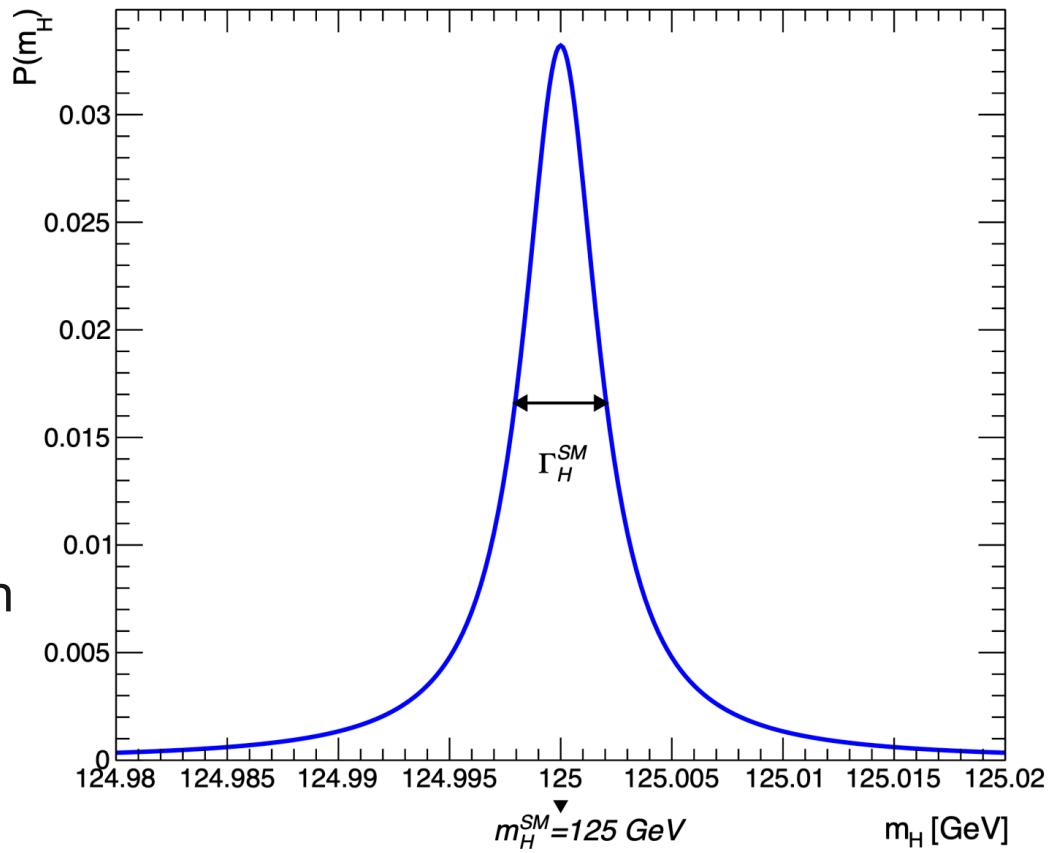

Mass

Mass: $H \to ZZ^* \to 4\ell$ analysis

- All production modes considered, major background is non-resonant ZZ^*
- Improved muon momentum-scale calibration (20% w.r.t. last Run 2 measurement)
- Deep neural network used to discriminate signal from background events
  - Inputs:
    $D_{ZZ^*} = \ln\left(|\mathscr{M}_{HZZ^*}|^2 / |\mathscr{M}_{ZZ^*}|^2 \right)$ and four-lepton system kinematics (p_{T} and η)
- Per-event $m_{4\ell}$ resolution obtained using dedicated neural network

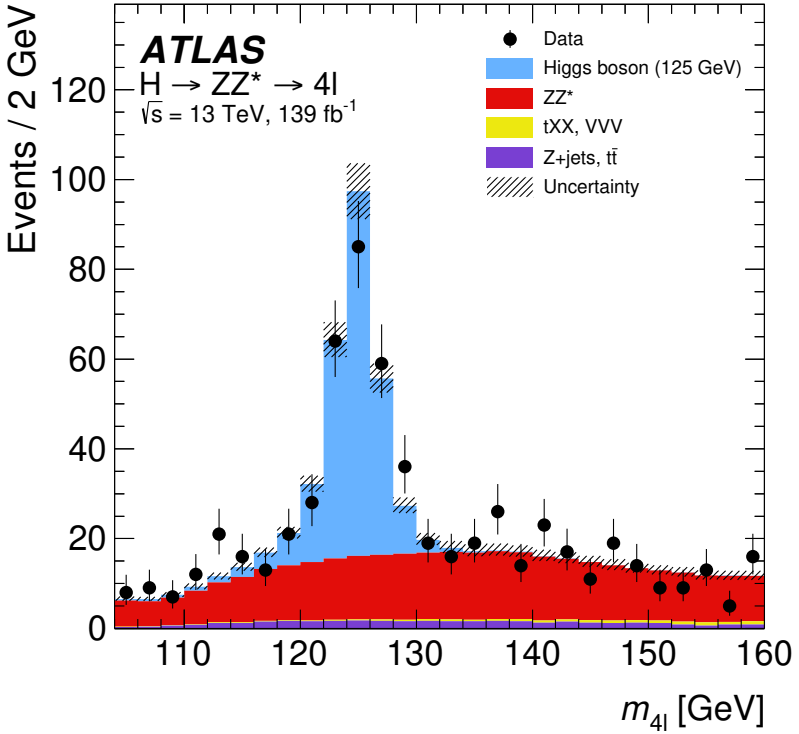

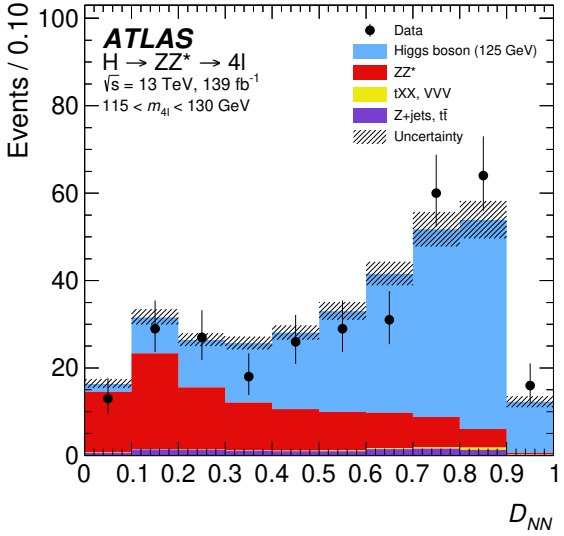

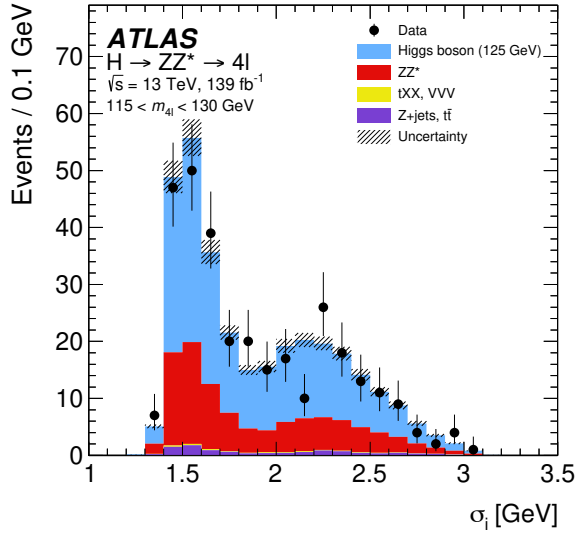

Mass: $H \to ZZ^* \to 4\ell$ results

- Results are statistically limited
- Mass extracted from simultaneous unbinned maximum-likelihood fit to the four subchannels in the mass range between 105 and 160 GeV: $(4\mu,\ 2e2\mu,\ 2\mu2e,\ 4e)$

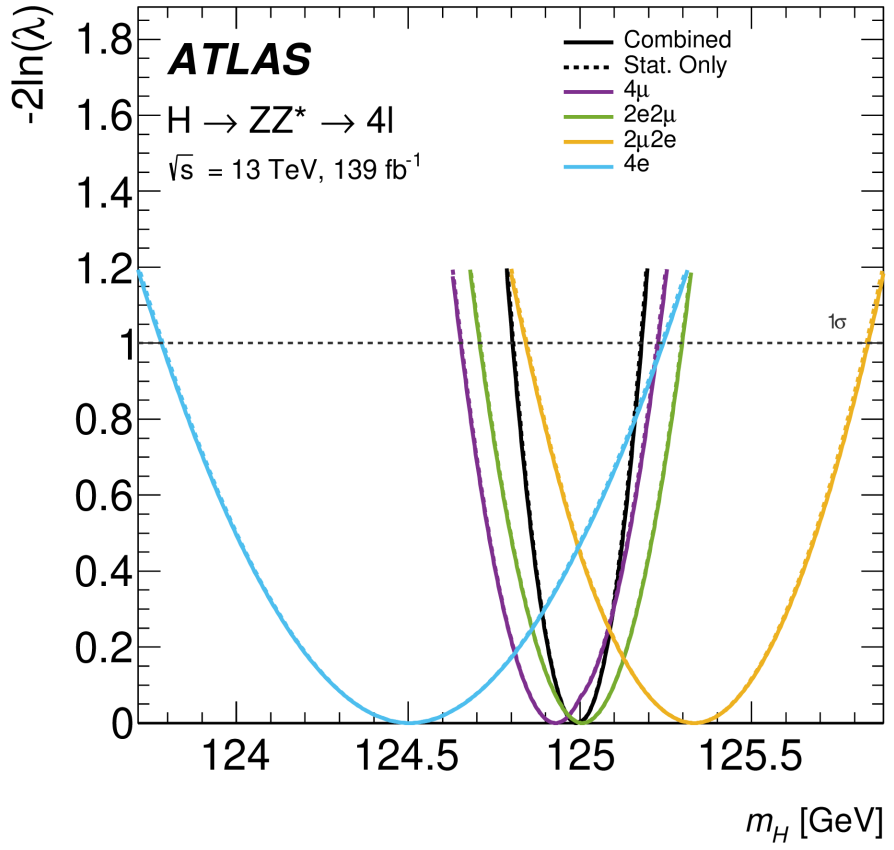

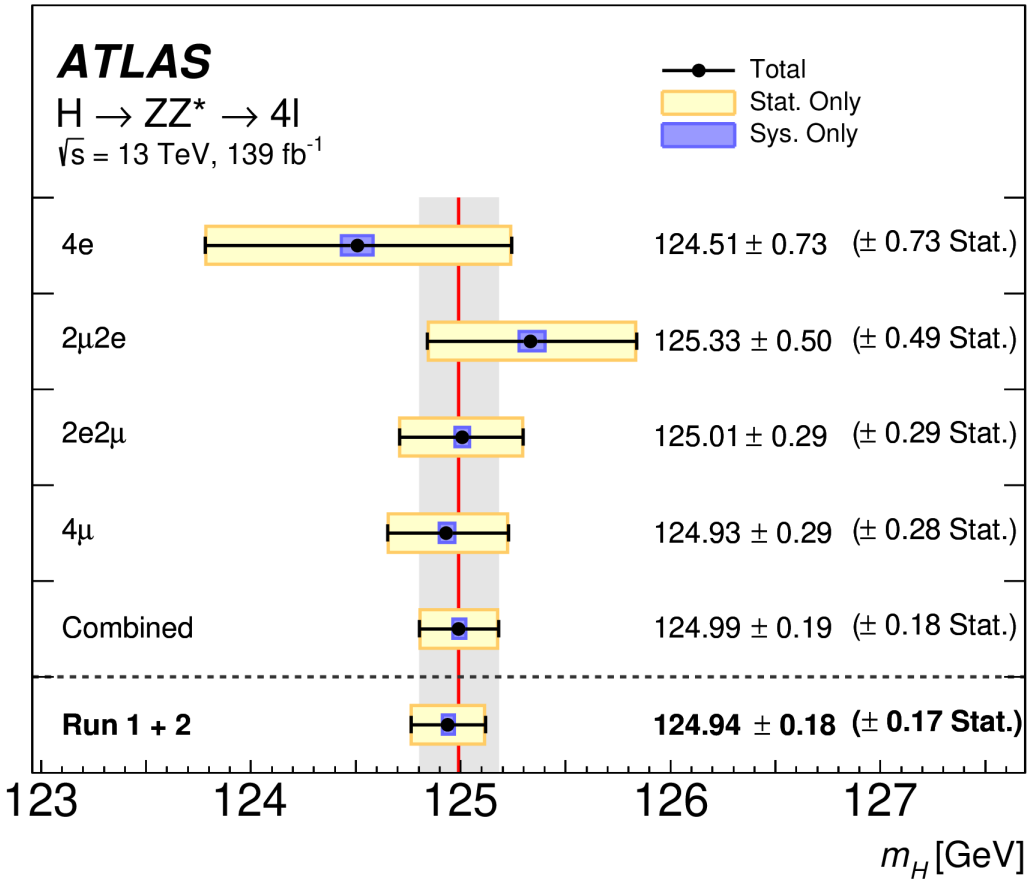

Systematic Uncertainty	Contribution [MeV]
Muon momentum scale	±28
Electron energy scale	±19
Signal-process theory	±14

Mass: $H \rightarrow \gamma\gamma$ analysis

- Exploiting new photon reconstruction with improved energy resolution and calibration
- Signal fit model uses a double-sided Crystal Ball function
- Fit uses 14 mutually exclusive categories optimized on photon phase space to reduce total uncertainty

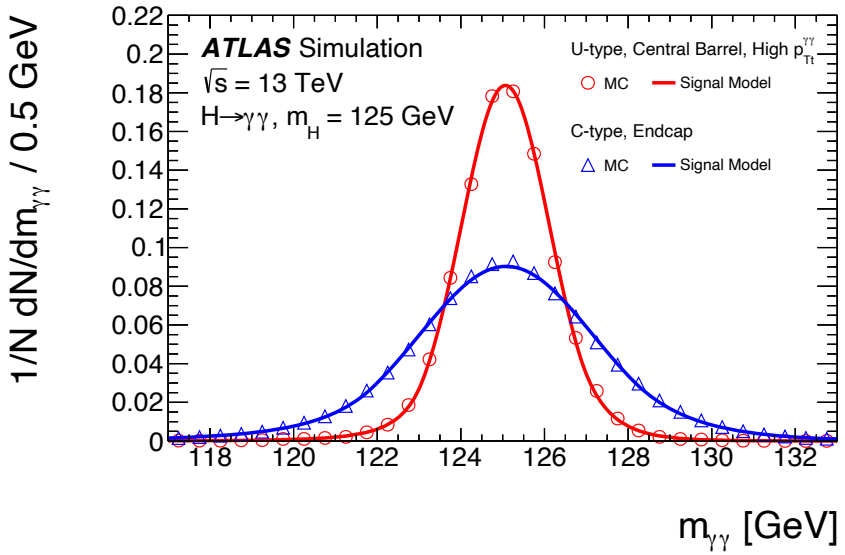

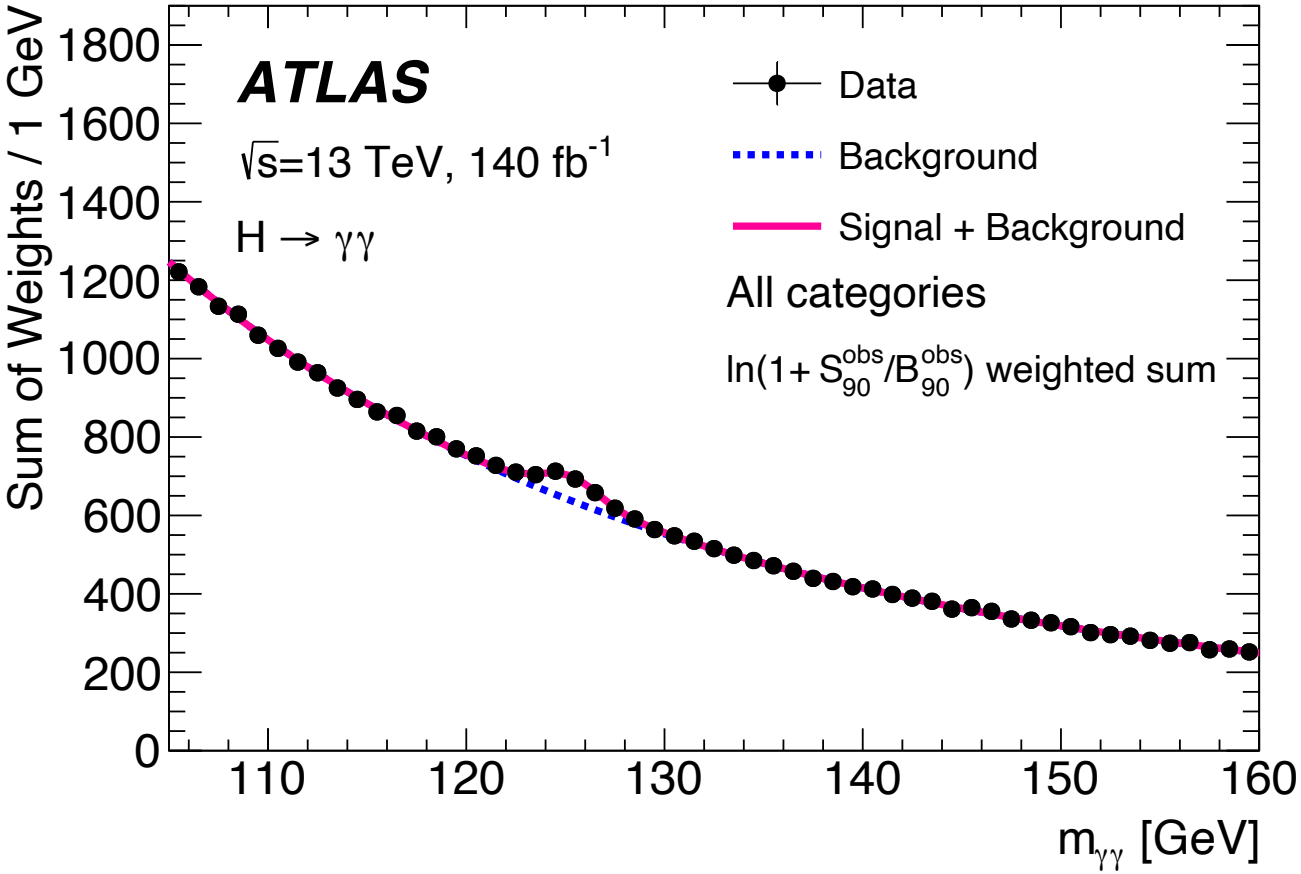

- Background fit model (exponential, power-law, or exponentiated second-order polynomial) chosen empirically for each category based on goodness of the fit on background MC templates

Mass: $H \to \gamma\gamma$ results

- Statistical uncertainty approaching level of systematic uncertainty; large improvements from refined calibration model
- 4x reduction of dominant systematic uncertainty (photon energy scale and resolution):
  320 MeV → 80 MeV

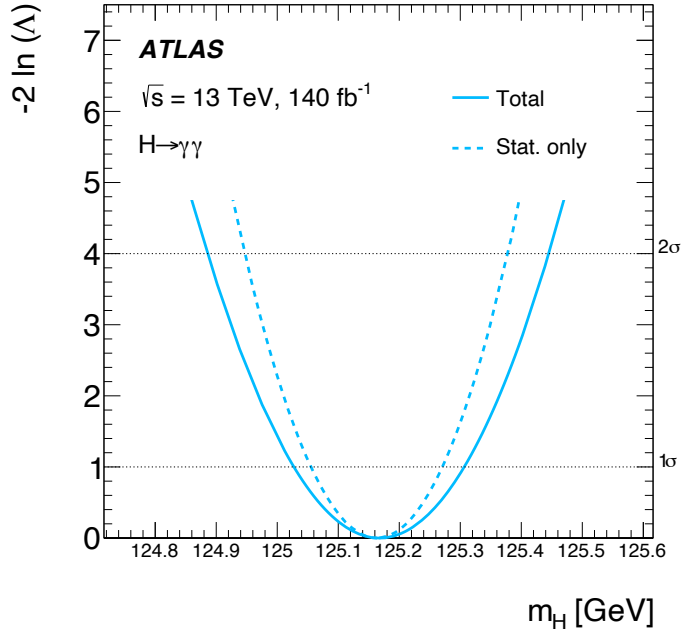

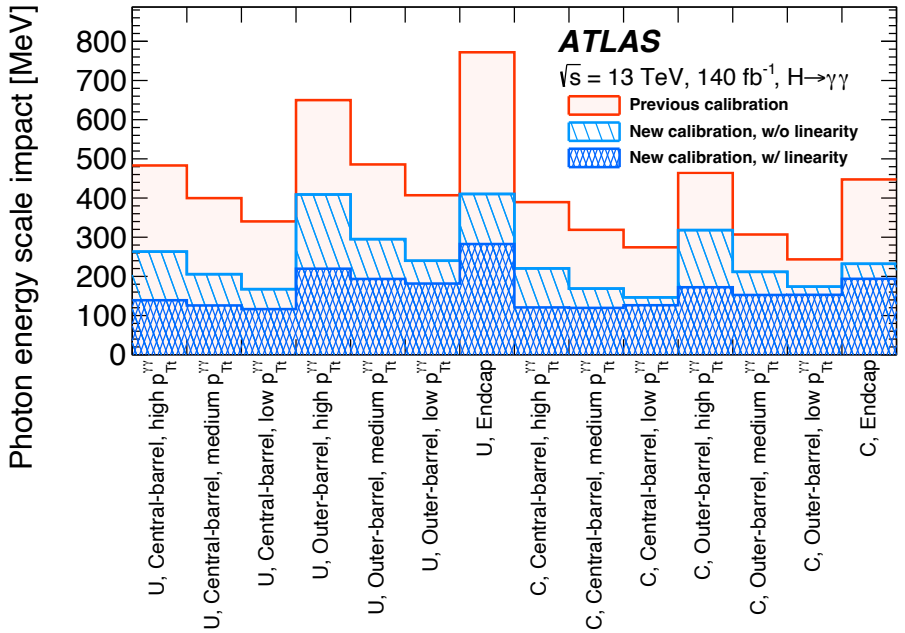

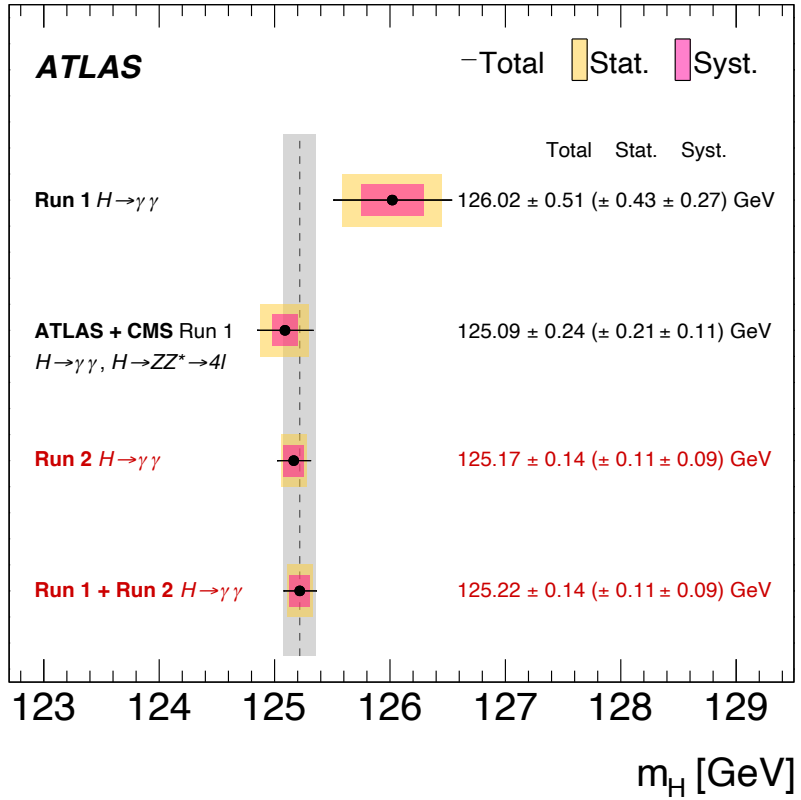

Source	Impact [MeV]
Photon energy scale	83
$Z \to e^+e^-$ calibration	59
E_T-dependent electron energy scale	44
$e^{\pm} \to \gamma$ extrapolation	30
Conversion modelling	24
Signal–background interference	26
Resolution	15
Background model	14
Selection of the diphoton production vertex	5
Signal model	1
Total	90

Mass: $H \to ZZ^* \to 4\ell$ and $H \to \gamma\gamma$ combination

- Both channels perform statistical combination with Run 1 with simultaneous fit on m_H

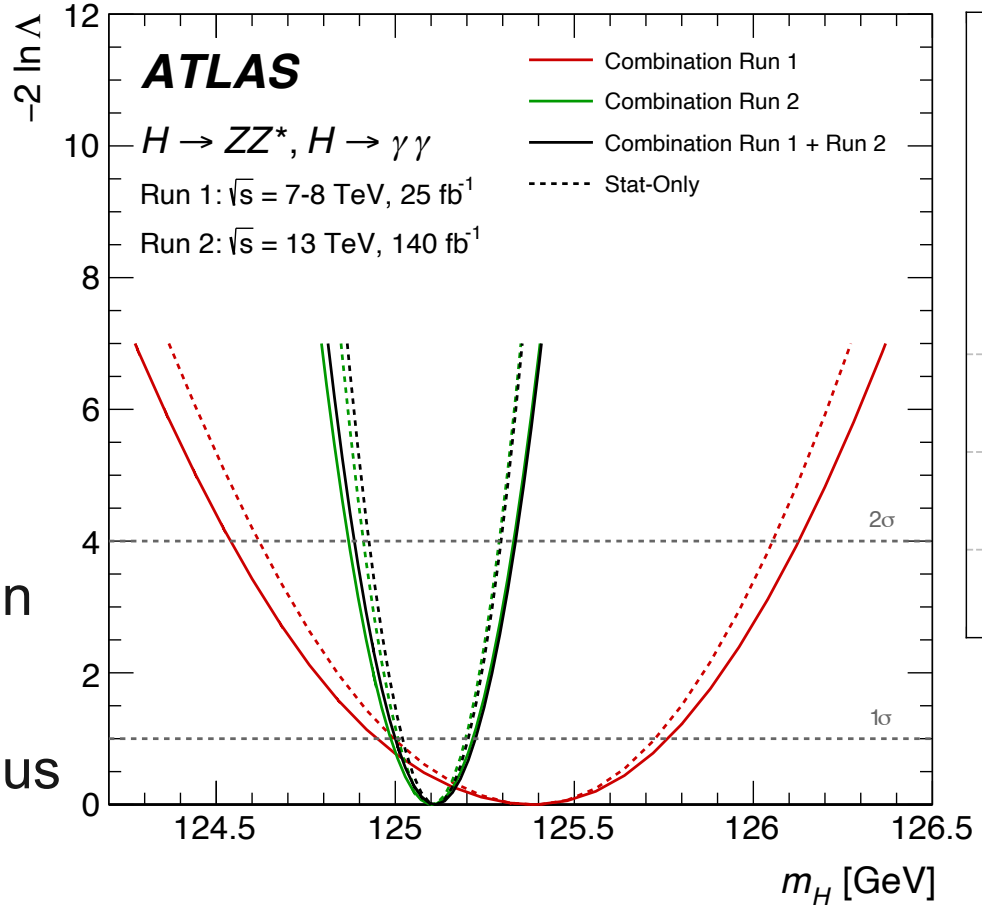

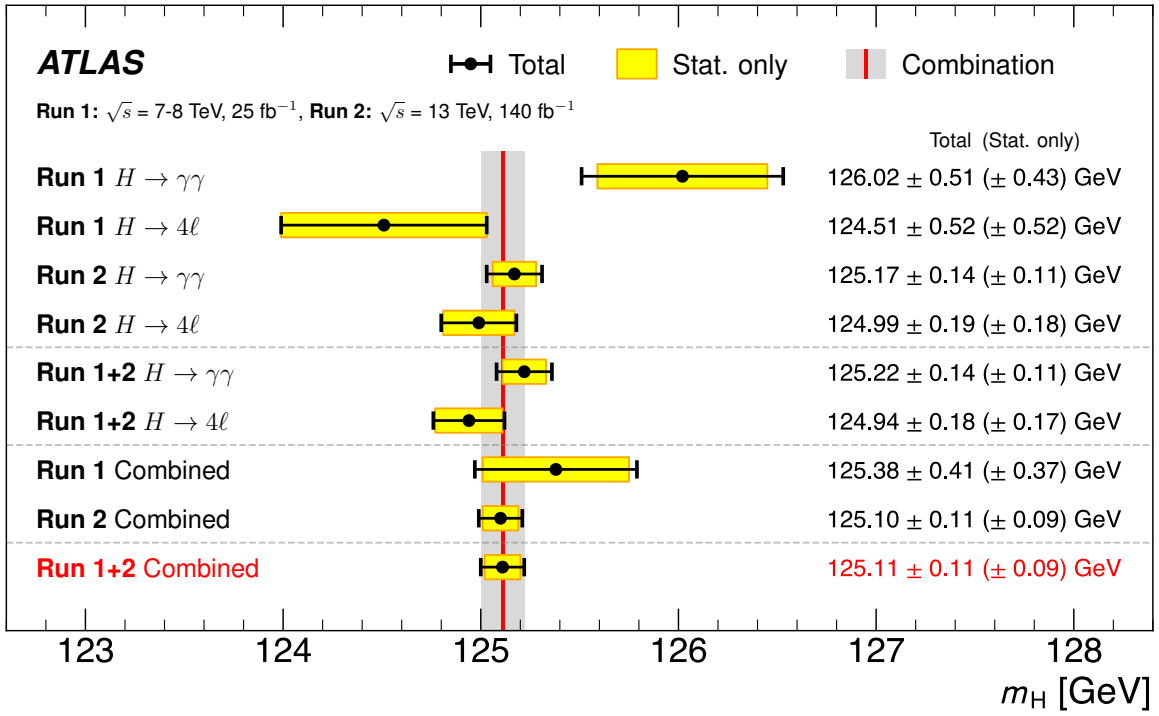

Source	Systematic uncertainty on m_H [MeV]
e/γ E_T-independent $Z \to ee$ calibration	44
e/γ E_T-dependent electron energy scale	28
$H \to \gamma\gamma$ interference bias	17
e/γ photon lateral shower shape	16
e/γ photon conversion reconstruction	15
e/γ energy resolution	11
$H \to \gamma\gamma$ background modelling	10
Muon momentum scale	8
All other systematic uncertainties	7

- 0.09% precision on the Higgs mass when combining both channels!

Width

Width: $H^* \to ZZ$ off-shell production analysis

- Include ggF and electroweak (EW) production $H^* \to ZZ$ signals, and their backgrounds with destructive interference
- Higgs boson width inferred by measuring ratio of off-shell to on-shell cross-sections
- Targeting two final states: 4ℓ and $2\ell 2\nu$

$$\sigma^{\text{on-shell}}_{gg\to H\to ZZ} \sim \frac{g^2_{ggF} g^2_{HZZ}}{m_H \Gamma_H}$$

$$\sigma^{\text{off-shell}}_{gg\to H\to ZZ} \sim \frac{g^2_{ggF} g^2_{HZZ}}{m^2_{ZZ}}$$

$$\Gamma_H \propto \frac{\sigma_{gg\to H^*\to ZZ}}{\sigma_{gg\to H\to ZZ^*}}$$

Eur. Phys. J. C (2015) 75:335

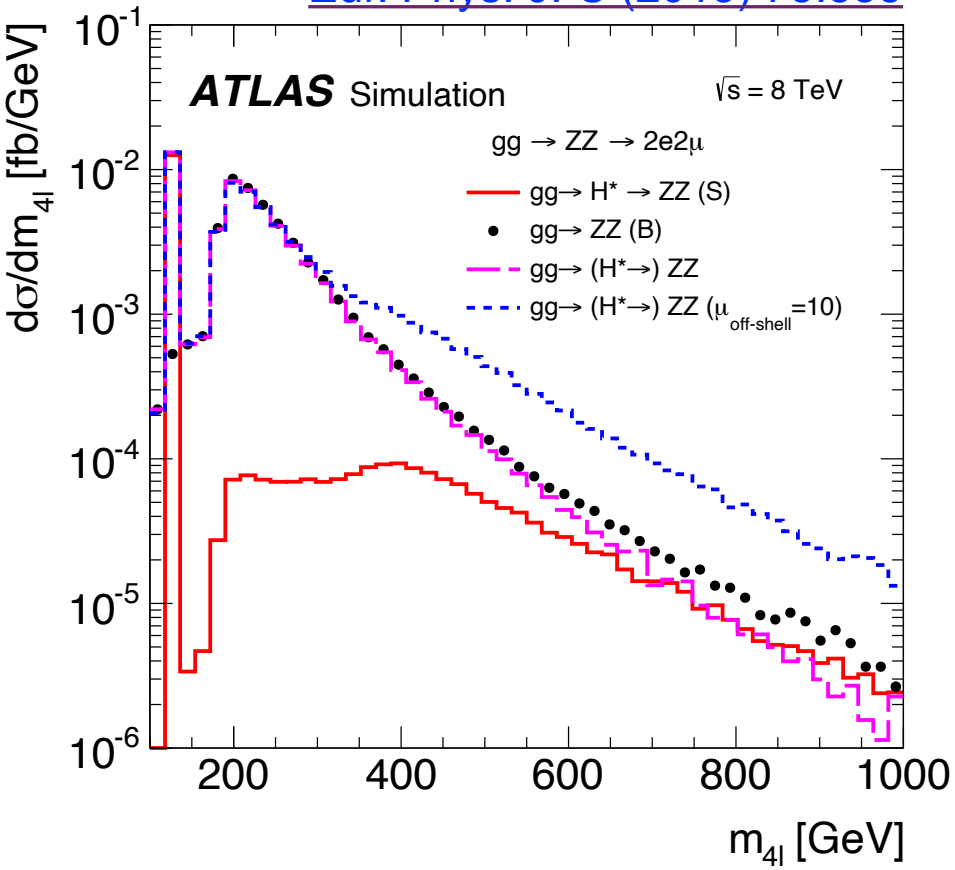

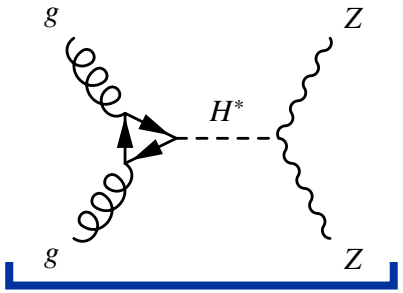

ggF signal

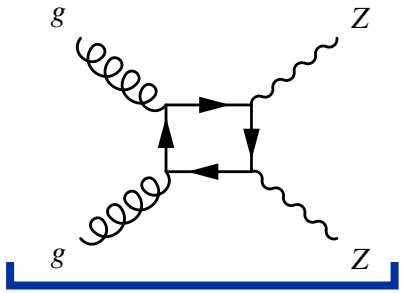

ggF background

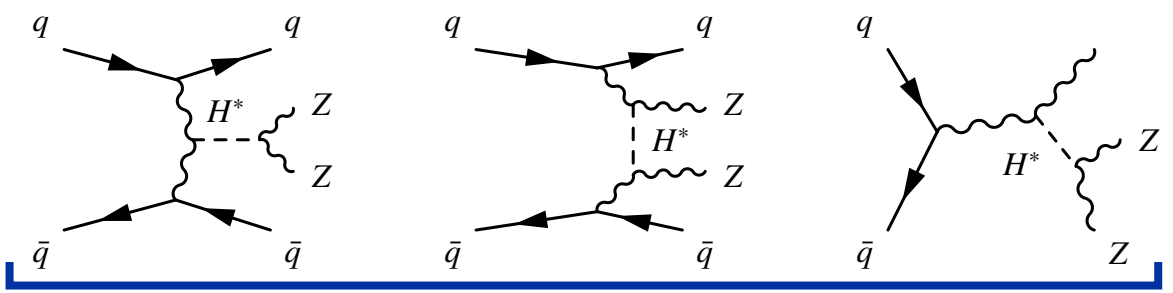

EW signal

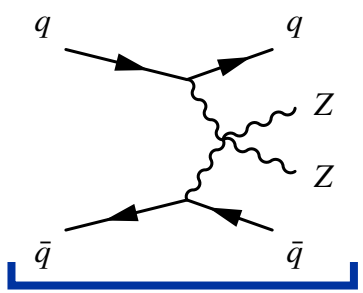

EW background

Width: $H^* \to ZZ$ off-shell production, 4ℓ channel

- Use multi-class neural network (NN) to enhance signal sensitivity;
  - NN differentiates among three event classes: off-shell Higgs boson signal (S), interfering background (B), non-interfering background (NI)
- Three signal regions (SR) are defined after requiring $m_{4\ell} > 220$ GeV:
  - EW: require two or more jets with $p_{\mathrm{T}} > 30$ GeV, $|\Delta\eta_{\mathrm{jj}}| > 4$
  - Mixed: require exactly one jet with $|\eta_{\mathrm{j}}| > 2.2$
  - ggF: remaining events

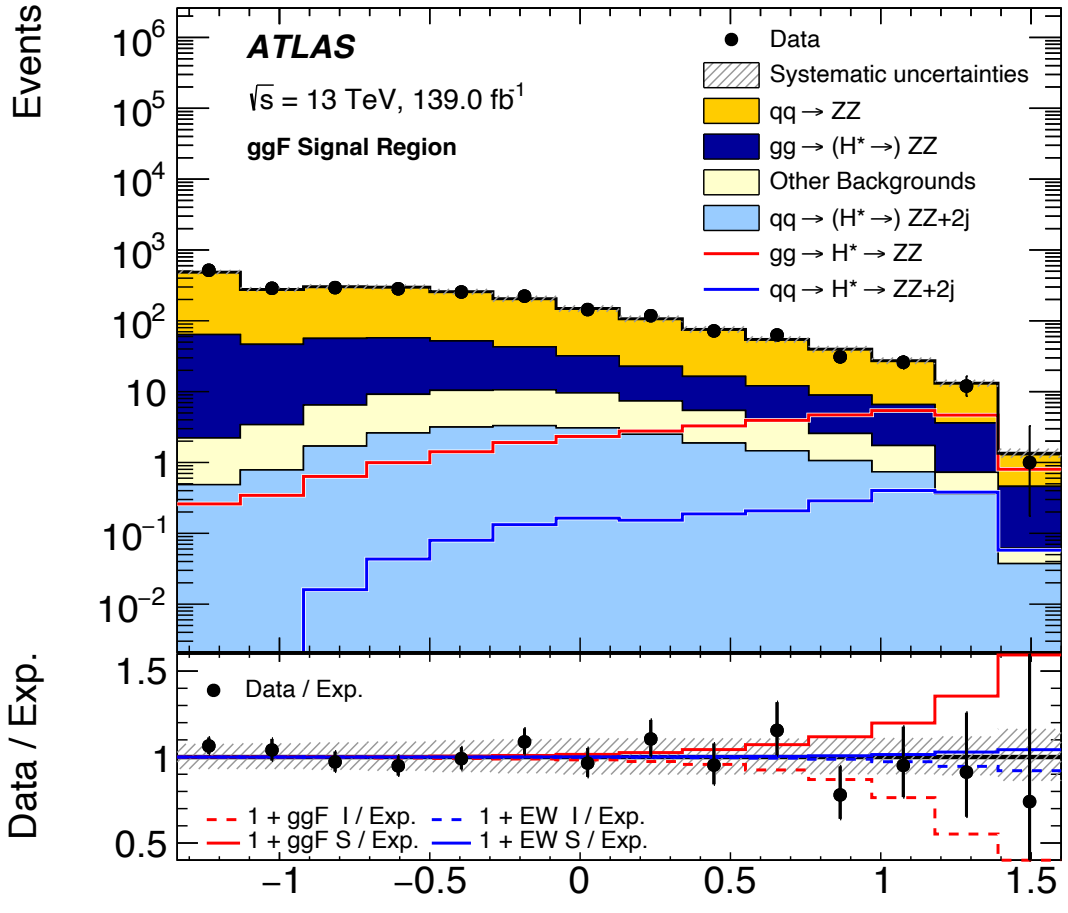

$$O_{\mathrm{NN}} = \log_{10}\left(\frac{P_{\mathrm{S}}}{P_{\mathrm{B}} + P_{\mathrm{NI}}}\right)$$

Width: $H^* \to ZZ$ off-shell production, $2\ell 2\nu$ channel

- Use m_{T}^{ZZ} as discriminating variable
- Require a pair of isolated leptons and $E_{\mathrm{T}}^{\mathrm{miss}} > 120$ GeV, then define three signal regions in the same way as for the 4ℓ channel
- Dedicated event selection to reduce contributions from WZ, $Z+$ jets, and nonresonant dilepton background processes

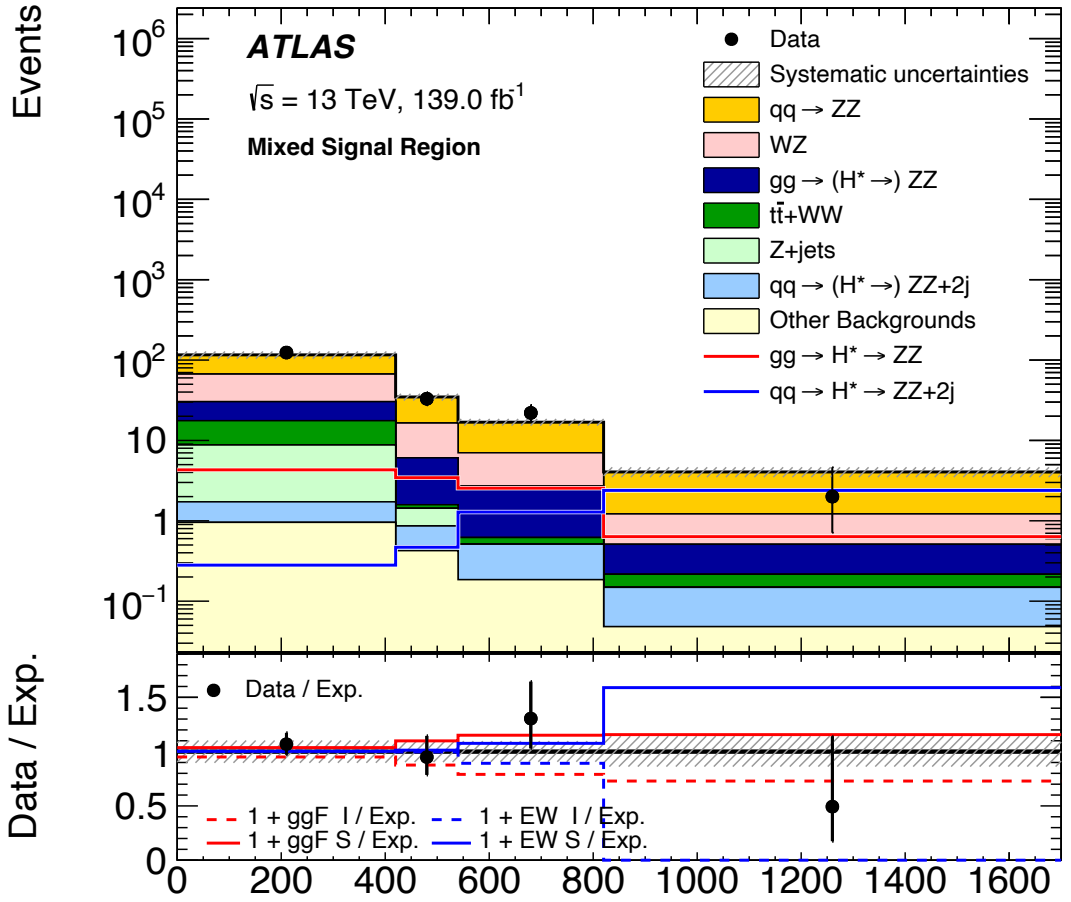

$$m_{\mathrm{T}}^{ZZ} \equiv \sqrt{\left[\sqrt{m_Z^2 + \left(p_{\mathrm{T}}^{\ell\ell}\right)^2} + \sqrt{m_Z^2 + \left(E_{\mathrm{T}}^{\mathrm{miss}}\right)^2}\right]^2 - \left|\vec{p}_{\mathrm{T}}^{\,\ell\ell} + \vec{E}_{\mathrm{T}}^{\mathrm{miss}}\right|^2}$$

Width: $H^* \rightarrow ZZ$ off-shell production results

- Simultaneously fit signal strength and background normalization factors in all signal regions and control regions
- Direct measurement of off-shell signal strength
- Combined with on-shell measurement to measure Γ_H with correlated (uncorrelated) experimental (theoretical) systematic uncertainties
- Observed $\Gamma_H = 4.5^{+3.0}_{-2.5}$ MeV

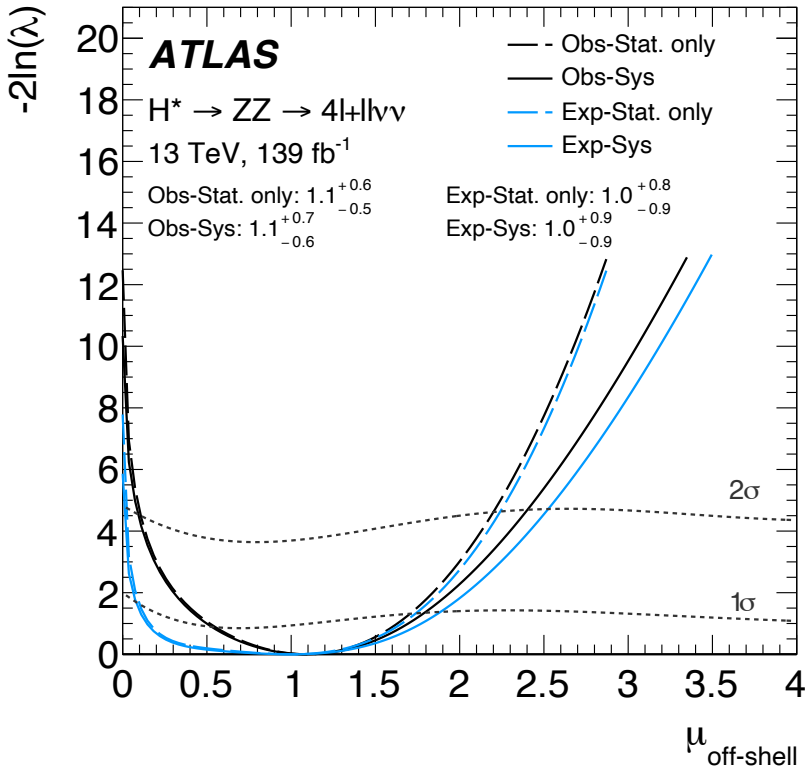

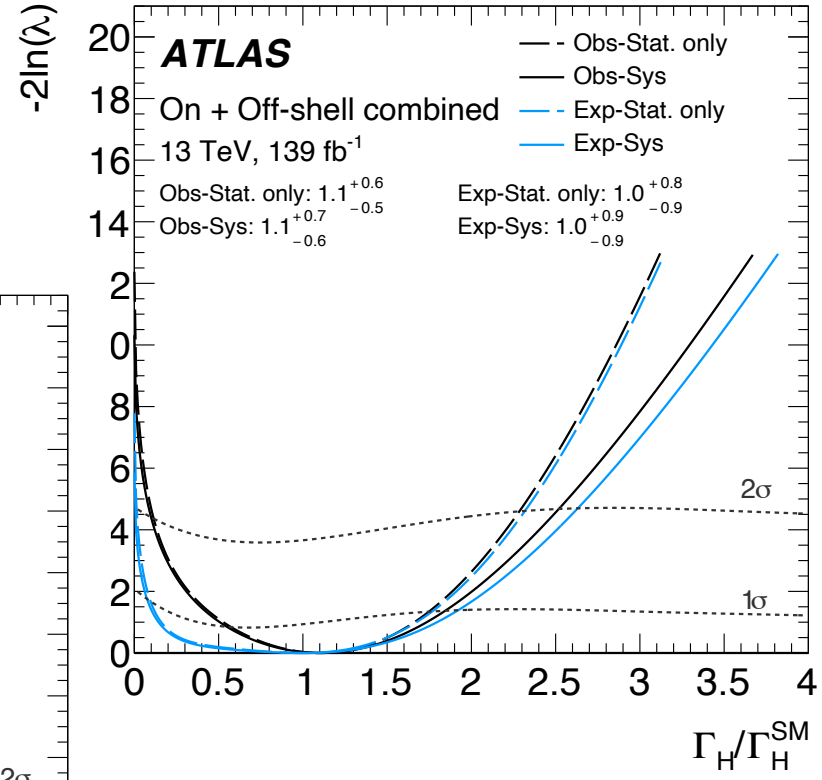

CP

CP: $H \to ZZ^* \to 4\ell$ analysis setup

- Goal is to probe the coupling strength of CP-odd operators (i.e. operators that lead to CP violation) and carry out differential cross-section measurements
- Build optimal observables (*OO*) for each EFT coupling (three for each basis and one for common parameterization $\tilde{d}$), depending on fitted variable
- 4 VBF signal regions based on output score of a three-class neural network discriminant trained to distinguish between VBF, VH, and ggF events

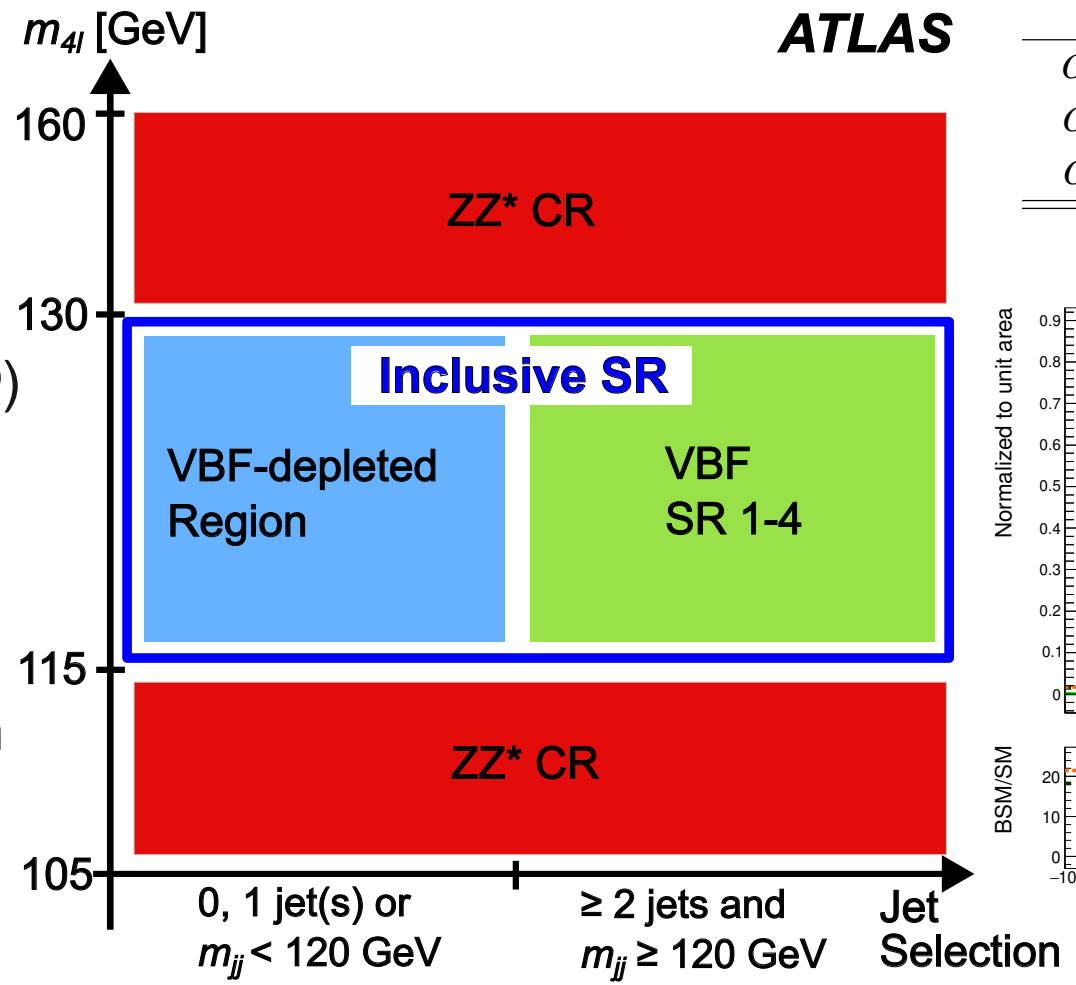

Operator	Structure	Coupling
	Warsaw Basis	
$O_{\Phi\tilde{W}}$	$\Phi^\dagger\Phi\tilde{W}^I_{\mu\nu}W^{\mu\nu I}$	$c_{H\widetilde{W}}$
$O_{\Phi\tilde{W}B}$	$\Phi^\dagger\tau^I\Phi\tilde{W}^I_{\mu\nu}B^{\mu\nu}$	$c_{H\widetilde{W}B}$
$O_{\Phi\tilde{B}}$	$\Phi^\dagger\Phi\tilde{B}_{\mu\nu}B^{\mu\nu}$	$c_{H\widetilde{B}}$
	Higgs Basis	
$O_{hZ\tilde{Z}}$	$hZ_{\mu\nu}\tilde{Z}^{\mu\nu}$	$\widetilde{c}_{zz}$
$O_{hZ\tilde{A}}$	$hZ_{\mu\nu}\tilde{A}^{\mu\nu}$	$\widetilde{c}_{z\gamma}$
$O_{hA\tilde{A}}$	$hA_{\mu\nu}\tilde{A}^{\mu\nu}$	$\widetilde{c}_{\gamma\gamma}$

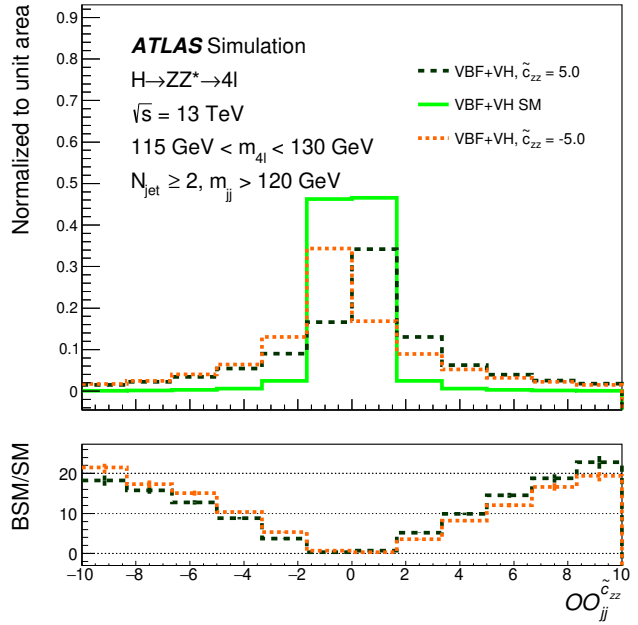

CP: $H \to ZZ^* \to 4\ell$ analysis

- Maximum-likelihood fit performed for CP-odd coupling parameters

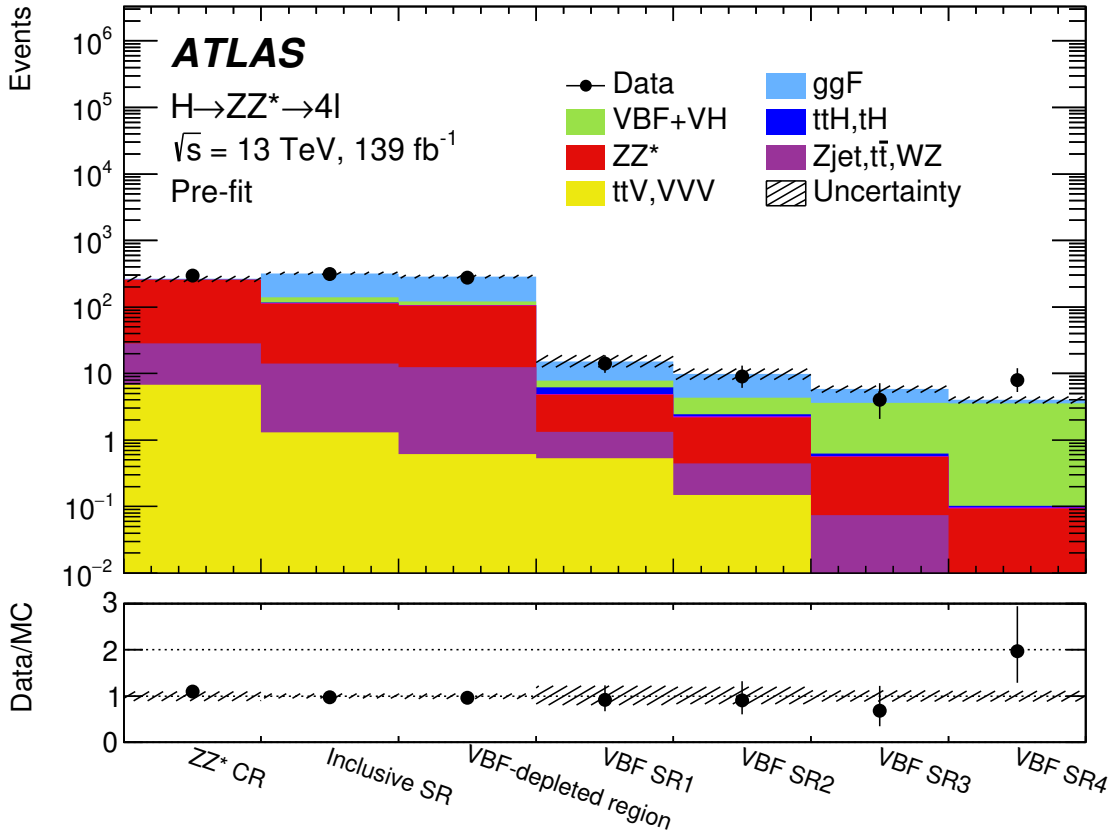

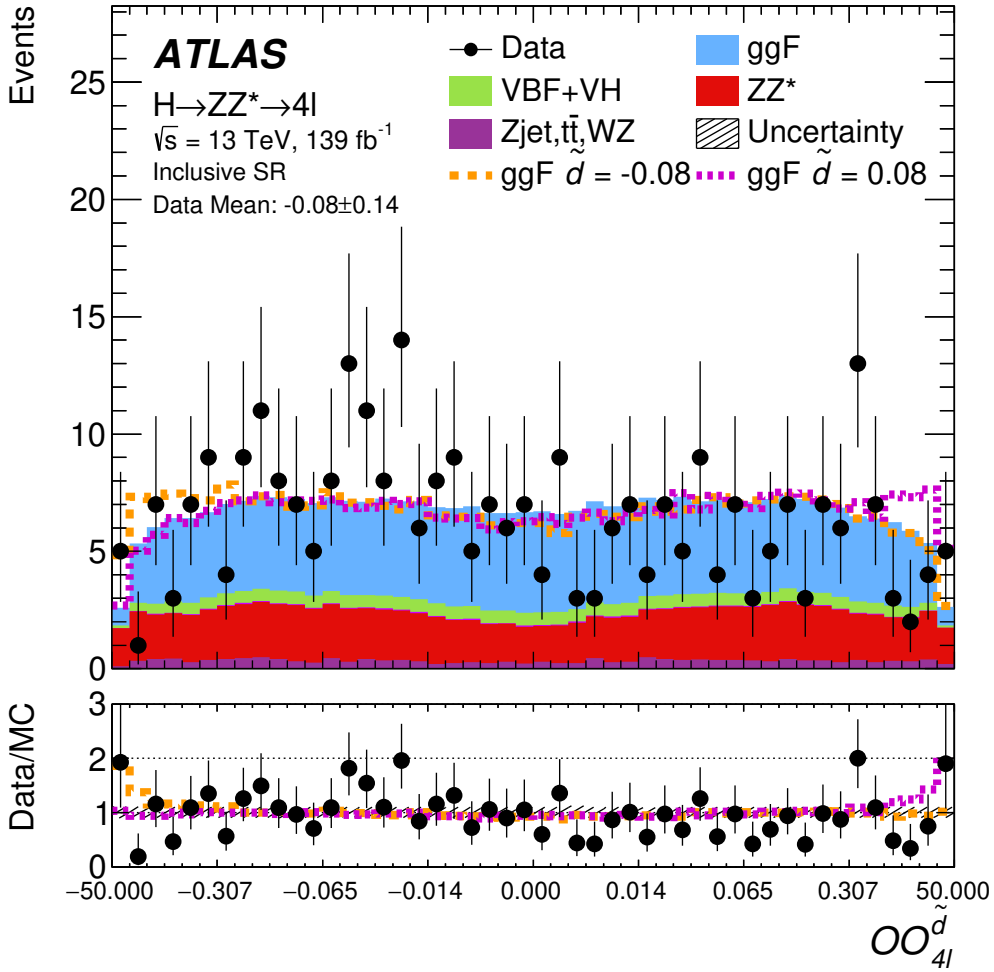

- Good agreement between data and SM expectation; mean value of observables for data are compatible with zero, indicating that the data exhibit no measurable asymmetry

CP: $H \to ZZ^* \to 4\ell$ results

- Constrain coupling parameters by scanning individually and in 2D

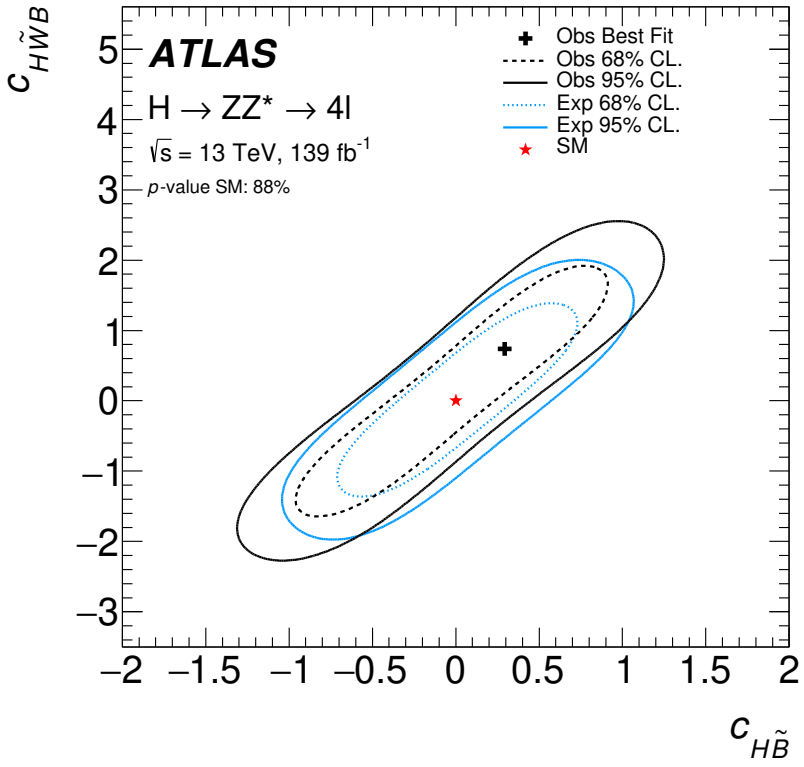

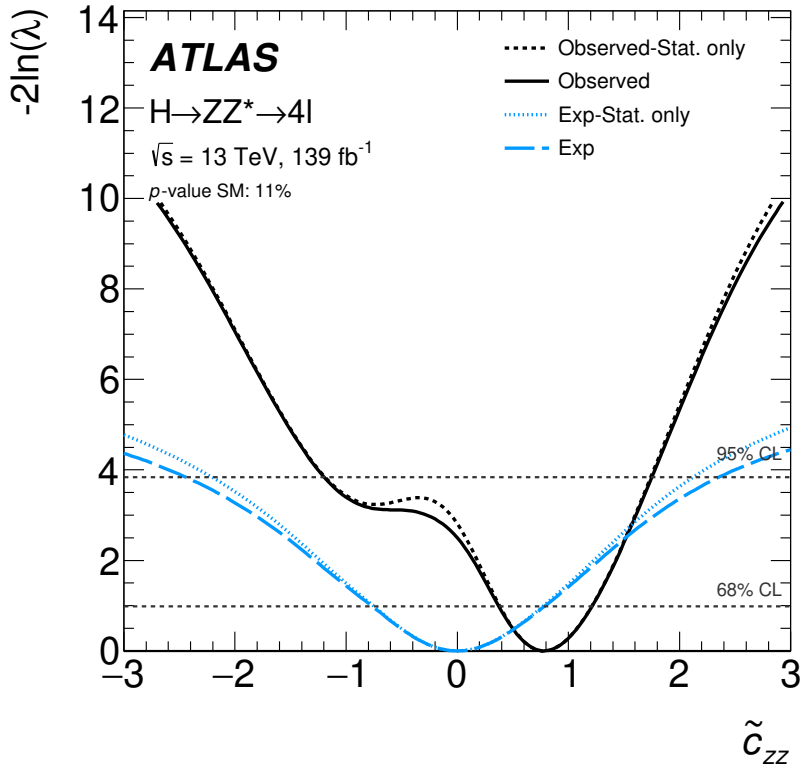

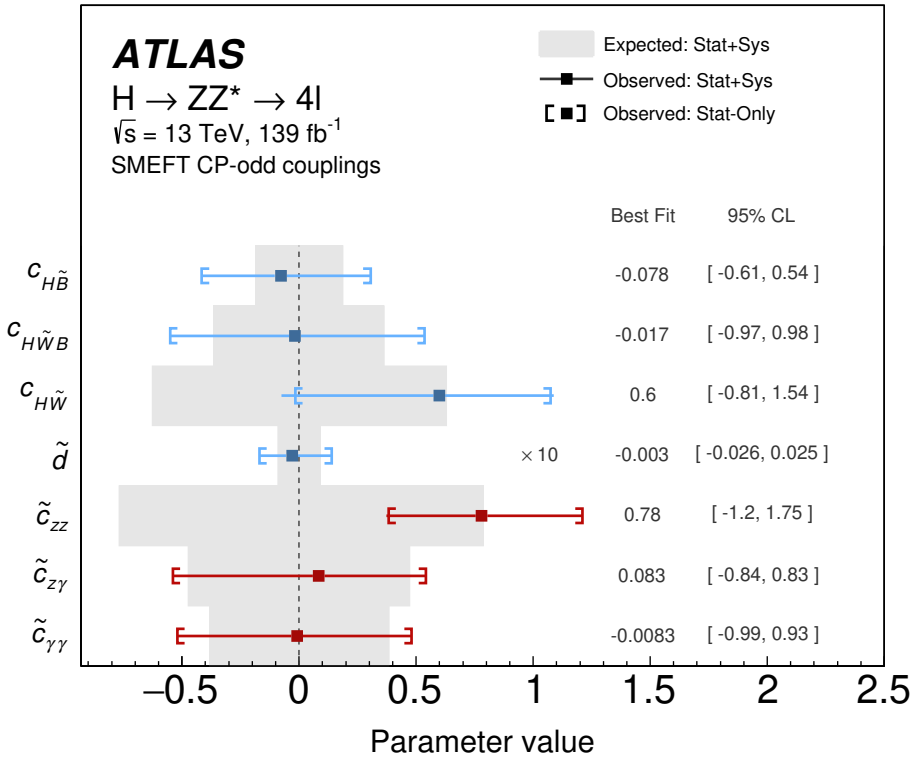

- Constraints consistent with SM predictions so far

CP: $H \to ZZ^* \to 4\ell$ differential results

- Differential cross-section measurements are performed for both production and decay
- Signal strength extracted by fitting the $m_{4\ell}$ spectrum in each bin
- Fiducial cross-sections measured in 3 bins in the $|\eta_{jj}| - m_{jj}$ plane

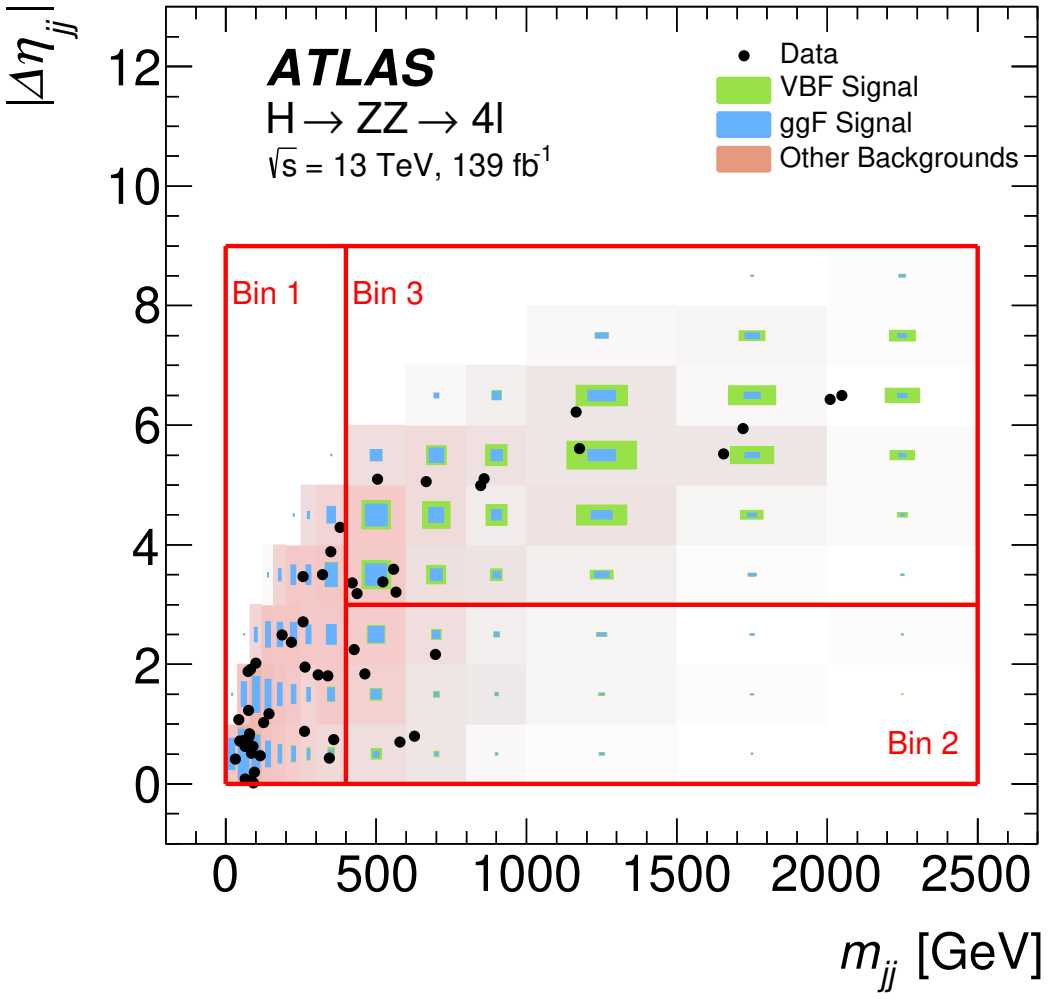

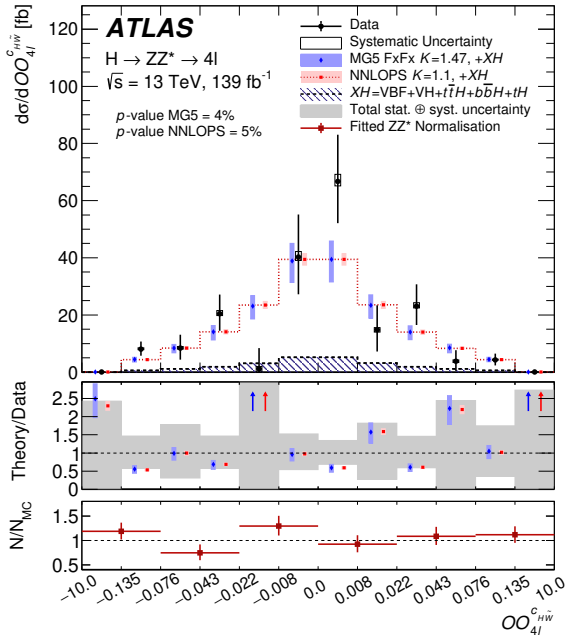

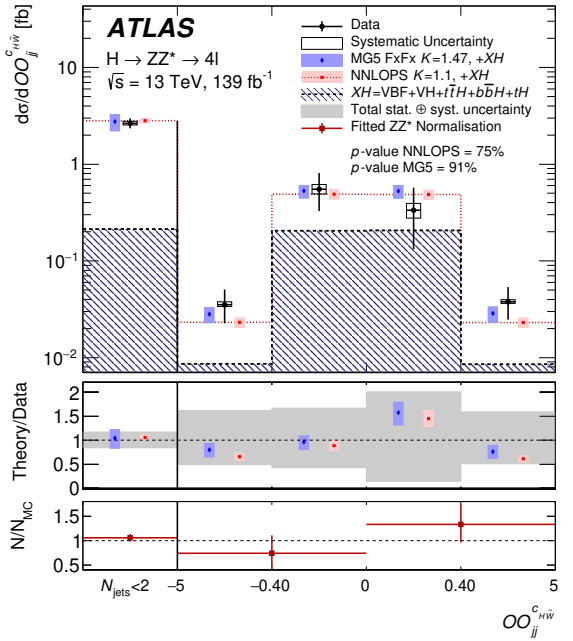

Summary & outlook

- Tremendous progress has been made in measuring the Higgs boson's properties since its discovery 12 years ago
  - Mass measured to precision of 0.09%
  - Width measurements honing in on true value
  - CP structure of Higgs couplings increasingly constrained
- Still only at the early stages of exploring the Higgs sector, with many more improvements and data still to come

Stay tuned for many more exciting results!

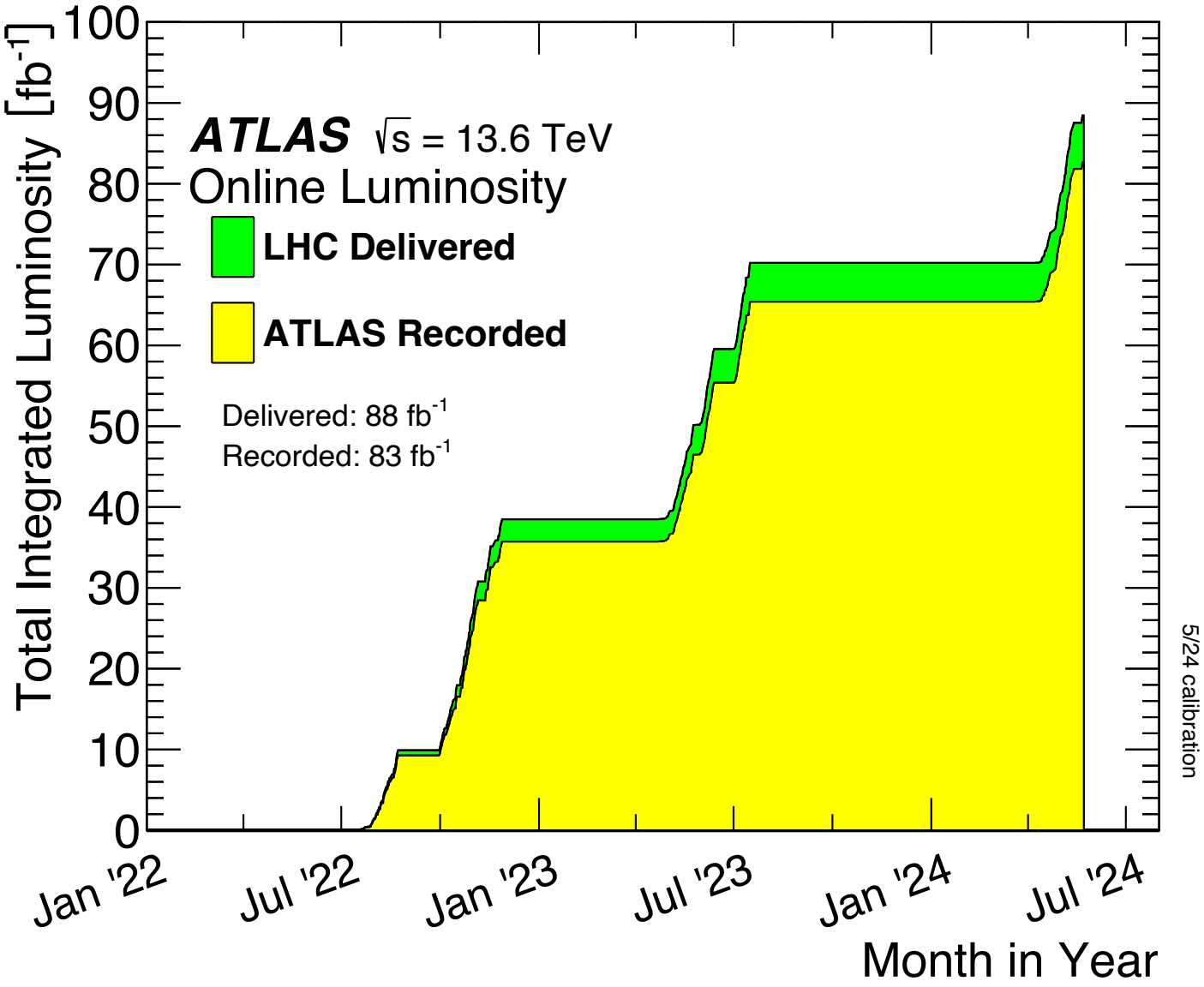

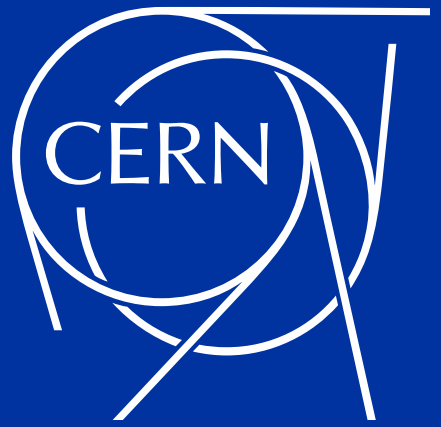

Thank you!
Merci!

Questions?

Bourses postdoctorales
Banting
Postdoctoral Fellowships

UCL

Mass: $H \rightarrow \gamma\gamma$ analysis categories

	Central-barrel	Outer-barrel	Endcap
C-type (>0 γ_{conv})	high p_{Tt}	high p_{Tt}	
	medium p_{Tt}	medium p_{Tt}	
	low p_{Tt}	low p_{Tt}	
U-type (0 γ_{conv})	high p_{Tt}	high p_{Tt}	
	medium p_{Tt}	medium p_{Tt}	
	low p_{Tt}	low p_{Tt}	

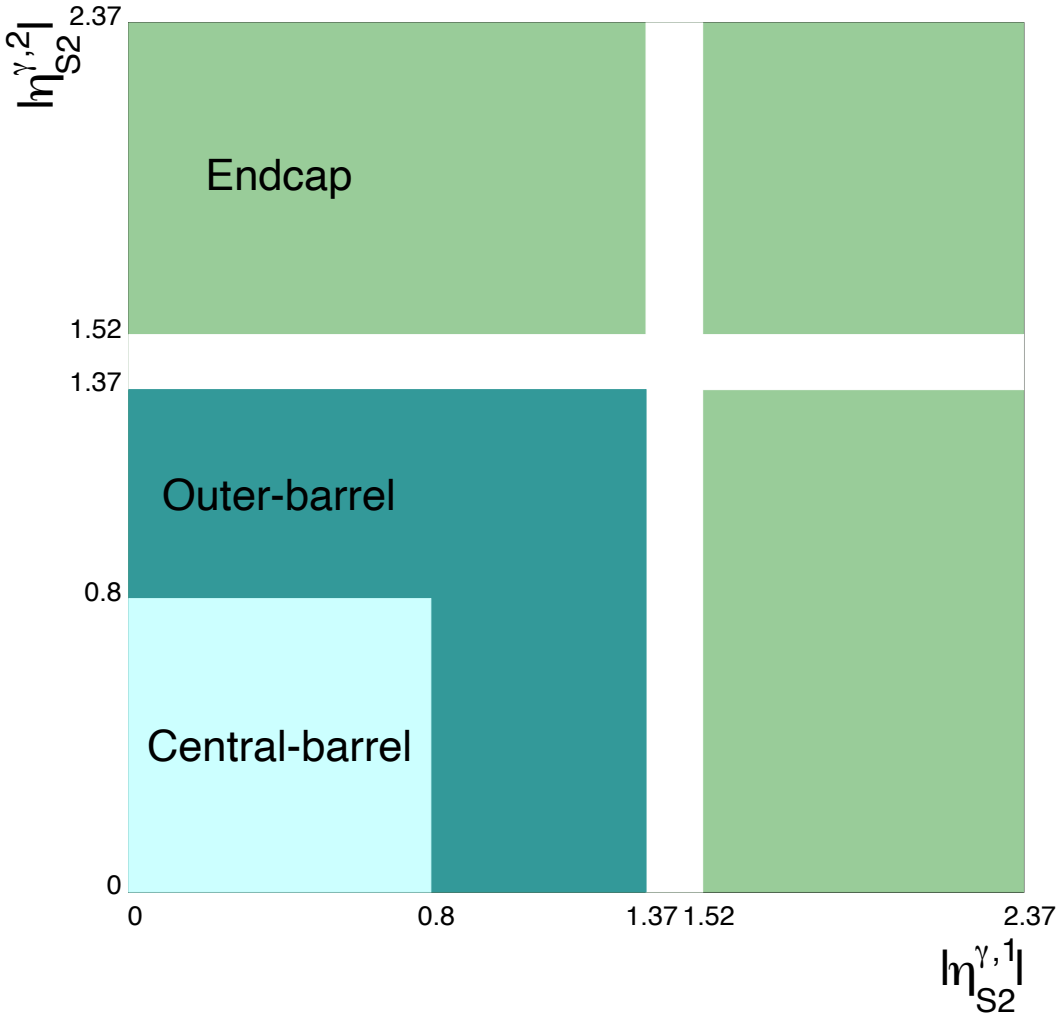

Mass: $H \to \gamma\gamma$ analysis categories (continued)

To increase the precision of the mass measurement, the selected events are classified into 14 categories with different signal-to-background ratios, diphoton invariant mass resolutions and photon energy scale uncertainties. The observables and the thresholds used to define the categories are optimised by minimising the expected total Higgs boson mass uncertainty for $m_H = 125.09$ GeV using a simplified version of the maximum-likelihood fit described in the next section, including the statistical uncertainties and the dominant systematic uncertainties from the photon energy scale calibration. The final choice of observables and thresholds for the categories used in the measurement is the following:

- The number of reconstructed converted photon candidates: events with no photon conversion candidates ('U'-type events) are considered separately from events with one or two $\gamma \to e^+e^-$ candidates ('C'-type events).
- The absolute value of the pseudorapidity $|\eta_{S2}|$ of each of the two energy clusters reconstructed in the electromagnetic calorimeter and associated with the photon candidates. The pseudorapidity η_{S2} is determined from the position of the barycentre of the cluster in the second sampling layer of the calorimeter and from the origin of the ATLAS coordinate system. Both the U-type and C-type events are separated into three subsamples: 'central barrel' (both photons have $|\eta_{S2}| < 0.8$), 'outer-barrel' (both photons have $|\eta_{S2}| < 1.37$ and at least one of these has $|\eta_{S2}| \geq 0.8$), and 'endcap' (at least one photon has $1.52 \leq |\eta_{S2}| < 2.37$).
- The magnitude $p_{\mathrm{Tt}}^{\gamma\gamma} = |\vec{p}_{\mathrm{T}}^{\,\gamma\gamma} \times \hat{t}|$ of the component of the diphoton transverse momentum that is orthogonal to the thrust axis, defined as $\hat{t} = (\vec{p}_{\mathrm{T}}^{\,\gamma_1} - \vec{p}_{\mathrm{T}}^{\,\gamma_2})/|\vec{p}_{\mathrm{T}}^{\,\gamma_1} - \vec{p}_{\mathrm{T}}^{\,\gamma_2}|$. Low ($p_{\mathrm{Tt}}^{\gamma\gamma} < 70$ GeV), medium (70 GeV $< p_{\mathrm{Tt}}^{\gamma\gamma} < 130$ GeV) and high ($p_{\mathrm{Tt}}^{\gamma\gamma} > 130$ GeV) $p_{\mathrm{Tt}}^{\gamma\gamma}$ categories are defined for U-type and C-type central-barrel and outer-barrel events.

Width: $H^* \rightarrow ZZ$ off-shell production statistics

- Why are the 1σ and 2σ lines wavy?
  - Confidence intervals are built based on the Neyman construction, as opposed to using the “usual' asymptotic approximation
  - Short answer, “toys”

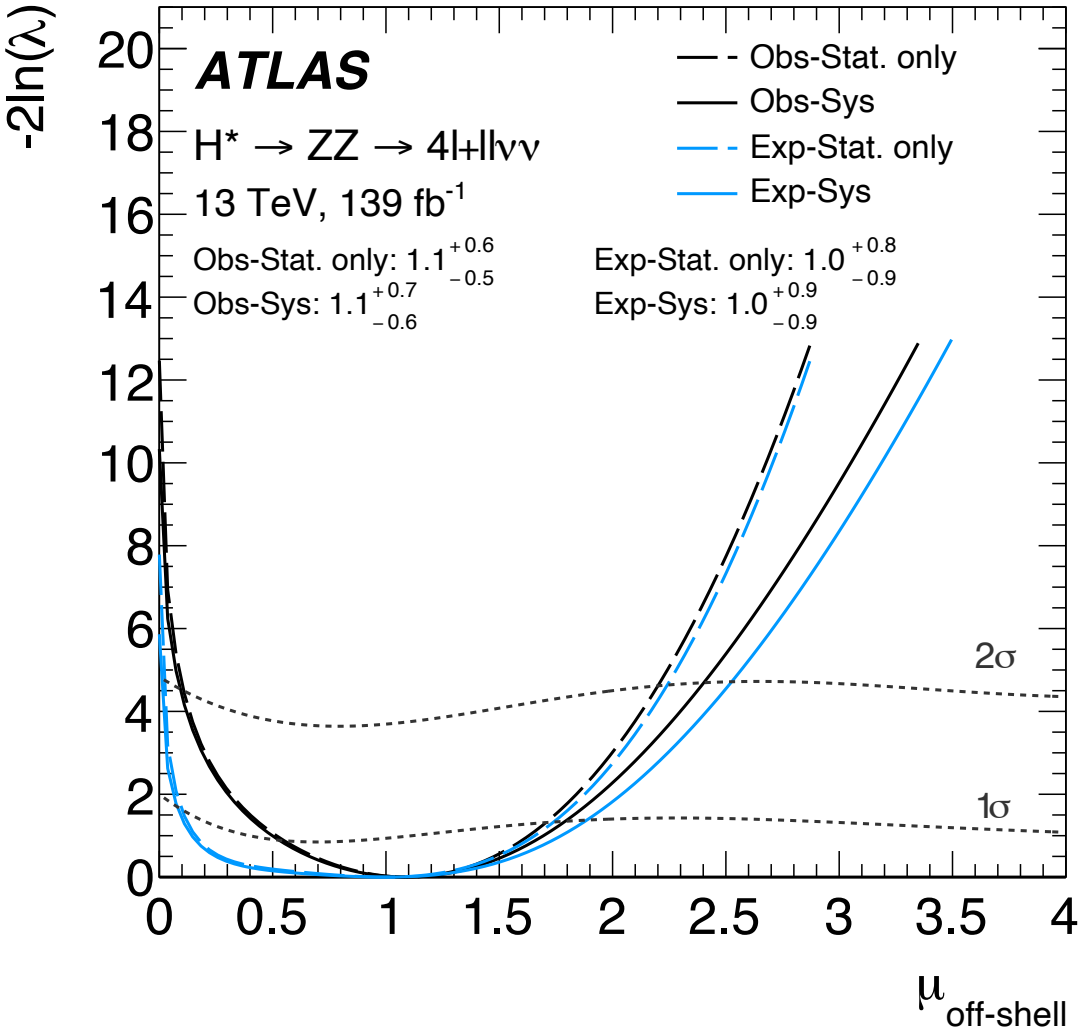

Width: $H^* \rightarrow ZZ$ off-shell production control regions

- 8 background normalization factors in total:
  - three ZZ CRs in 0, 1, 2+ jets
  - three WZ CRs in 0, 1, 2+ jets
  - one emu CR
  - one Z+jets CR